TISSUE-SPECIFIC PROGENITOR AND STEM CELLS

STEM CELLS
TRANSLATIONAL MEDICINE

Intranasal delivery of mesenchymal stem cell-derived extracellular vesicles exerts immunomodulatory and neuroprotective effects in a 3xTg model of Alzheimer's disease

Morris Losurdo[1] | Matteo Pedrazzoli[2] | Claudia D'Agostino[1] | Chiara A. Elia[3,4] |
Francesca Massenzio[2] | Elena Lonati[1] | Mario Mauri[1] | Laura Rizzi[1] |
Laura Molteni[1] | Elena Bresciani[1] | Erica Dander[5] | Giovanna D'Amico[5] |
Alessandra Bulbarelli[1,6] | Antonio Torsello[1] | Michela Matteoli[3,7] |
Mario Buffelli[2] | Silvia Coco[1,6]

[1]School of Medicine and Surgery, University of Milano-Bicocca, Monza, Italy

[2]Department of Neurosciences, Biomedicine and Movement Sciences, University of Verona, Verona, Italy

[3]Laboratory of Pharmacology and Brain Pathology, Neuro Center, Humanitas Clinical and Research Center—IRCCS, Rozzano (MI), Italy

[4]CNR, Institute of Neuroscience, Milano, Italy

[5]Centro Ricerca Tettamanti, Pediatric Department, University of Milano-Bicocca, Fondazione MBBM, Monza, Italy

[6]NeuroMI-Milan Center for Neuroscience, University of Milano-Bicocca, Milano (MI), Italy

[7]Department of Biomedical Sciences, Humanitas University, Pieve Emanuele (MI), Italy

Correspondence
Silvia Coco, PhD, School of Medicine and Surgery, University of Milano-Bicocca, Via Cadore 48, Monza 20900, Italy.
Email: silvia.coco@unimib.it

Abstract

The critical role of neuroinflammation in favoring and accelerating the pathogenic process in Alzheimer's disease (AD) increased the need to target the cerebral innate immune cells as a potential therapeutic strategy to slow down the disease progression. In this scenario, mesenchymal stem cells (MSCs) have risen considerable interest thanks to their immunomodulatory properties, which have been largely ascribed to the release of extracellular vesicles (EVs), namely exosomes and microvesicles. Indeed, the beneficial effects of MSC-EVs in regulating the inflammatory response have been reported in different AD mouse models, upon chronic intravenous or intracerebroventricular administration. In this study, we use the triple-transgenic 3xTg mice showing for the first time that the intranasal route of administration of EVs, derived from cytokine-preconditioned MSCs, was able to induce immunomodulatory and neuroprotective effects in AD. MSC-EVs reached the brain, where they dampened the activation of microglia cells and increased dendritic spine density. MSC-EVs polarized in vitro murine primary microglia toward an anti-inflammatory phenotype suggesting that the neuroprotective effects observed in transgenic mice could result from a positive modulation of the inflammatory status. The possibility to administer MSC-EVs through a noninvasive route and the demonstration of their anti-inflammatory efficacy might accelerate the chance of a translational exploitation of MSC-EVs in AD.

KEYWORDS

Alzheimer's disease, dendritic spines, extracellular vesicles, inflammation, mesenchymal stem cells, microglia

1 | INTRODUCTION

Alzheimer's disease (AD), the most common form of age-related dementia, is characterized by a slow progressive and detrimental degeneration of the central nervous system (CNS). Neuropathological hallmarks of AD are extracellular β-amyloid plaques, neurofibrillary tangles, inflammation, synaptic and neuronal dysfunction, and degeneration.[1] Inflammation, a concurrent etiopathological mechanisms in AD, is primarily orchestrated by microglia, which represent the innate immune cells of the CNS. They exert also regulatory roles on synaptic plasticity, interacting with neurons by cell-to-cell contact or by secreting mediators,[2,3] thus contributing to the remodeling of neural circuits and being involved in learning and memory processes.[4]

In order to rapidly respond to minimal changes of brain microenvironment, microglia are plastically capable of adopting different and complex activation states, which allow them to contribute either to the cytotoxic response, or to injury resolution and tissue repair.[5,6]

In AD, an unbridled microglia activity can exacerbate tau pathology,[7] mediate synapse loss,[8] and enhance the secretion of pro-inflammatory mediators,[9,10] driving—directly and/or indirectly—neuronal injury.[11] Importantly, genome-wide association studies have shown that most of the identified AD-risk genes are selectively or preferentially expressed by microglia cells,[12] highlighting the relevance of immune genes for the development of the disease and implicating microglia dysfunction as a contributing factor of AD pathogenesis.[13]

Therefore, targeting neuroinflammation is becoming one of the promising therapeutic interventions at which researchers are aiming at. In this context, mesenchymal stem/stromal cells (MSCs) due to their immunoregulatory abilities are raising a lot of interest. Indeed, MSCs, fibroblastoid multipotent stem cells, turned out to be endowed with therapeutic potential in different CNS pathologies, including AD[14-18] contributing to restore tissue homeostasis in a pleiotropic manner.[19,20] Extracellular vesicles (EVs), heterogeneous membrane surrounded-structures ranging approximately from 40 nm to 1 μm, have been identified as key players in cellular communication among many cell types,[19-22] and are emerging as critical mediators of many of MSC actions, including immunomodulation[23,24] (for a review, see Reference 25). EVs are powerful carriers, which differ in origin, size, and shape, largely displaying the functions of the cells they origin from.[26] Interestingly, various ex vivo preconditioning strategies, such as cytokine stimulation, are being exploited to increase MSC anti-inflammatory abilities.[27-30] Noteworthy, such approaches also boost the release of highly immunomodulant EVs that successfully target inflammatory and oxidative processes in different pathological contexts, including AD.[31-33] So far, the in vivo studies investigating MSC-EV beneficial effects in AD models have exploited chronic treatments (weeks/months), primarily administering EVs via systemic route[32] or by intracerebroventricular (ICV) injection[33,34] showing either partial rescue of the pathology[32,33] or a preventive action in reducing the Aβ plaque burden and the amount of dystrophic neurites.[34] In our study, we tested, for the first time, the efficacy of the intranasal injection of cytokine-preconditioned MSC-EVs in 3xTg AD mice. Our results show that EVs dampen microglia activation and reduce dendritic spine loss.

Significance statement

In the attempt to find a possible cure for Alzheimer's disease (AD), mesenchymal stem cells (MSCs) and their derived extracellular vesicles (EVs) are being investigated for therapeutic purposes thanks to their protective and anti-inflammatory properties. The results from this study show that MSC-EVs operate in dampening inflammation (that favors and accelerates the pathogenic process in AD) and in inducing neuroprotective effects. Furthermore, they sustain the delivery of MSC-EVs through the intranasal route, being safe and low invasive, thus laying the foundation for a translational future exploitation of MSC-EVs toward therapy.

We hypothesize that these effects may be due to EV anti-inflammatory actions.

2 | MATERIALS AND METHODS

2.1 | Isolation and culture of MSCs

After informed consent was obtained, MSCs were isolated from bone marrow of healthy donors, plated at 800×10^3 cells/cm^2 and expanded in vitro in low glucose Dulbecco's modified Eagle's medium (DMEM; Lonza, Basel, Switzerland) containing 10% fetal bovine serum (FBS; Biosera, Dubai, UAE), 2 mM L-glutamine, and 1% penicillin/streptomycin (Lonza), as previously described[35] (for further details, see Supporting Information).

2.2 | Ex vivo preconditioning and characterization of MSCs

For preconditioning, MSC growth medium was replaced with fresh serum-free (SF)-DMEM for 24 or 48 hours with the addition of TNFα (20 ng/mL) and IFNγ (25 ng/mL) (Peprotech, Rocky Hill, New Jersey; SF+CYT). Untreated MSCs were incubated with SF-DMEM without the addition of pro-inflammatory cytokines.

For MSC characterization after cytokine treatment, cells were plated at a density of 1000 cells/cm^2. Differentiation potential of preconditioned MSCs (pMSCs) was assessed by evaluating the commitment toward osteogenic and adipogenic lineages.

2.3 | Isolation and characterization of preconditioned MSC-EVs

To isolate EVs (a pool of exosomes and microvesicles), serum-free MSC-conditioned medium (CM) was collected and subjected to a

modification of the widely used protocol by Théry et al.[36] Briefly, the medium derived from $\cong 7 \times 10^6$ MSCs was centrifuged to remove cells and cell debris. Then the supernatant was centrifuged at 4°C 110 000g for 70 minutes and the obtained EV pellet was resuspended in phosphate buffered saline (PBS; Lonza) and centrifuged at 4°C 110 000g for 70 minutes to remove soluble factor contaminants. Finally, EVs, recovered in the pellet, were resuspended in Eagle's minimal essential medium (MEM; Gibco, Thermo Fisher Scientific, Waltham, Massachusetts) or PBS for in vitro or in vivo experiments, respectively. EV quantification was performed by determination of the protein contents by bicinchoninic acid assay (BCA; Thermo Fisher Scientific). For size distribution and concentration, EVs were diluted in 1 mL of sterile PBS and subjected to nanoparticle tracking analysis (NTA) by NS300 instrument (Malvern, Worcestershire, UK; see also Reference 34).

3 | IN VITRO STUDIES

3.1 | Microglia cultures and experimental design

Primary cultures of microglial cells were isolated from mixed cultures of cortical and hippocampal astrocytes from 1 to 2 day postnatal brains of C57BL/6 mice. Briefly, after the removal of meninges, the isolated cortices and hippocampi were subjected to mechanical digestion and resuspended in complete glial medium (MEM, 20% FBS, 33 mM Glucose [Sigma-Aldrich, St. Louis, Missouri], 1% Na-Pyruvate, 2 mM L-ultra glutamine, 100 μg/mL streptomycin, and 100 U/mL penicillin [Lonza]) for plating. After reaching, the confluence microglial cells were harvested by shaking mixed glial cultures and seeded at a concentration of 200 000 cells/well on poly-ornithine (0.05 mg/mL) precoated 24-well plastic culture plates. To drive M1 phenotypic polarization, microglial cells were exposed to the pro-inflammatory stimuli (TNFα [20 ng/mL] and IFNγ [25 ng/mL])[37] after 24 hours from plating. Then, p-MSC-derived EVs (4.5 μg/mL) were administered to microglial cells (Figure S1).

3.2 | Enzyme-linked immunosorbent assay

For enzyme-linked immunosorbent assay (ELISA), supernatants were collected and the levels of interleukins IL-6, IL-1β, IL-10, and IL-4 were measured by a commercially available kit of ELISA (Peprotech), following manufacturer's instructions. Optical density values for cytokine concentration were acquired by Fluostar Omega microplate reader (BMG LABTECH, Offenburg, Germany).

3.3 | Western blot analyses

MSCs and microglial cells were lysed for the analysis of specific markers by Western Blotting (WB) (Table S1, "In vitro" column). Total protein amount (30 μg [for MSC] and 15 μg [for microglia]) was

measured by BCA and run on classical Sodium Dodecyl Sulphate - PolyAcrylamide Gel Electrophoresis (SDS-PAGE). All the data were normalized to β-actin, except for CD68 and CD206 microglial markers whose expression normalization was carried out with respect to the total amount of proteins detected by the Ponceau staining, allowing a straightforward correction for lane-to-lane variation.[38,39] For further information about WB procedures, see Supporting Information.

4 | IN VIVO STUDIES

4.1 | Animals

Procedures involving animals and their care were conducted in conformity with the EU guidelines (2010/63/UE) and Italian law (decree 26/14) and were approved by the University of Verona ethical committee and local authority veterinary service. For these experiments eight (four/group) 7-month female triple-transgenic AD mice (3xTg-AD) expressing three mutant human transgenes—PS1M146V, APPSwe, and tauP301L—were purchased from The Jackson Laboratory (Sacramento, California). All efforts to minimize animal suffering and number were made. Animal use was approved by the Italian Ministry of Health, in agreement with the EU Recommendation 2007/526/CE.

4.2 | Experimental design

EVs were resuspended in sterile PBS solution at a concentration of 300 μg/mL (30 μg corresponding vesicular protein, approximately 15×10^9 vesicles). Seven-month-old 3xTg female mice were anesthetized with isoflurane before being carefully intranasally administered with PBS solution or EVs in ∼5 μL spurts per nostril. Overall, each mouse received 100 μL of vehicle or EVs twice, each injection separated by 18 hours (50 μL/d). After 21 days, each mouse was anesthetized using the tribromoethanol drug (TBE; Sigma-Aldrich), and perfused transcardially with 0.1 M PBS followed by formaldehyde 10 vol%/vol%, buffered 4 wt%/vol% (Paraformaldehyde (PFA) 4%; Titolchimica, Rovigo, Italy), then processed for microglia activation and dendritic spine density (Figure S2). For EV tracking studies, mice injected with PKH26-labeled EVs (Sigma-Aldrich) were perfused and fixed 6 hours after the second intranasal administration.

4.3 | Immunofluorescence

Immunofluorescence (IF) was performed on 40 μm coronal sections of prefrontal cortex (from 2.40 to 2.80 mm Bregma), CA1 region of medial hippocampus (from −1.955 to −2.355 mm Bregma) and entorhinal cortex (from −2.80 to −3.30 mm Bregma). After masking the tissue aspecific binding sites by 30 minutes incubation with blocking solution (3% bovine serum albumin and 0.3% Triton X-100 [Sigma-Aldrich] in PBS), slices were processed O/N at 4°C with

different anti-mouse primary antibodies: (Table S1, "In vivo" column). Samples were acquired using a confocal laser scan microscope (Sp5, Leica). Fluorescent images were derived by z-stack projections (maximum intensity) of sections obtained with the open source software for image processing ImageJ (NIH, Bethesda, Maryland).

4.4 | Analysis of microglia activation

Microglia activation was investigated by evaluating the cell density and cell soma size. Microglia density was calculated as the total number of Iba-1+/4′,6-diamidino-2-phenylindole (DAPI) positive cells,

within the Z-projection acquired for each slice, by collecting stacks of 50 μm for a total volume of 0.0144 mm^3. Semiquantitative analysis, aiming at determining microglia cell soma size and expression of microglia markers, was performed using a specifically designed macro with ImageJ software (Supporting Information).

4.5 | Golgi-Cox staining

After fixation, each half of the brain was stained with Golgi-Cox solution (1% mercury chloride, 1% potassium dichromate, and 1% potassium chromate in distilled water)[40,41] and stored at Room Temperature (RT) in dark for 2 weeks. Then the brains were kept
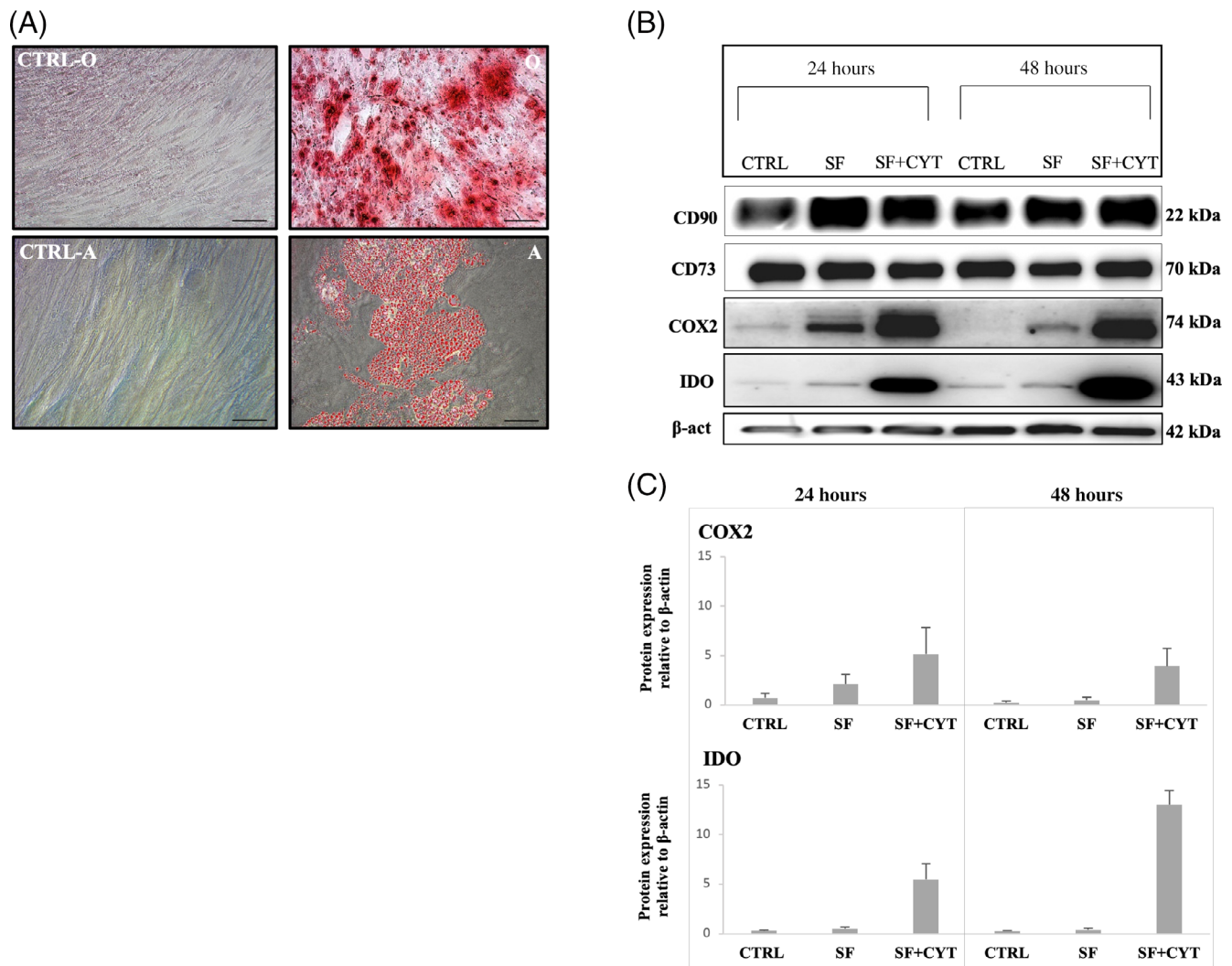

FIGURE 1 Cytokine preconditioning of MSCs (p6) in a SF-medium (SF+CYT) causes the upregulation of the immunomodulatory markers and preserves their stemness potential. A, MSCs were committed toward osteogenic (O) or adipogenic (A) lineages after the preconditioning protocol. Calcium deposits (O, in red) are visualized by Alizarin Red, while fat droplets (A, in red) are stained by Oil Red, indicating osteocytic and adipocytic differentiation, respectively. CTRL-O and CTRL-A: controls of MSCs grown in the absence of osteogenic (O) and adipogenic (A) inducing differentiation media. Images were acquired by phase contrast microscopy. Magnification ×20. Scale bars = 50 μm. B, Immunoblotting evaluation of the expression of typical stemness (CD90 and CD73) and immunoregulatory markers (COX2 and IDO) by MSCs subjected to SF + cytokine (SF+CYT) or SF preconditioning (CTRL: control; SF: serum-free; CYT: cytokines, TNFα and IFNγ). C, Histograms relative to the quantification of the immunomodulatory marker bands in (B). For the comparison between groups (SF+CYT at 24 and 48 hours) unpaired, two-tailed Student's t test was used. All the data are expressed as mean ± SEM (n = 3). MSC, mesenchymal stem cell; SF, serum-free

in 30% PBS sucrose solution for 24 hours in order to reduce the tissue fragility during the sectioning procedure.[42] After collection of 100-μm-thick slices of hippocampus, prefrontal, and entorhinal cortices using vibratome (Leica VT1200, Leica Biosystems, Germany), they were processed with Kodak Developer and Fixer (GBX Carestream Dental, Congers, New York) for 5 minutes and 15 minutes, respectively, and washed in distilled water for 5 minutes after each step. Finally, slices were dehydrated using increasing concentrations of ethanol (50%-60%-75%-85%) and mounted on slides with coverslips using Eukitt (Sigma-Aldrich).[43]

4.6 | Dendritic spine analysis

Images were collected using an Olympus BX63 microscope (Olympus Corporation, Japan) and acquired by the Neurolucida 64-Bit software (MBF Bioscience, Williston, North Dakota). Acquisition of dendritic spines in CA1 region of medial hippocampus, prefrontal, and entorhinal cortices occurred at 100×. We collected images of 117 × 88 μm and analyzed three slices per mice at the Bregma points mentioned above, with each stack being acquired using a z-stack unit of 0.35 μm. Images were deconvolved through AutoQuant software, converted in 8-bit images and,
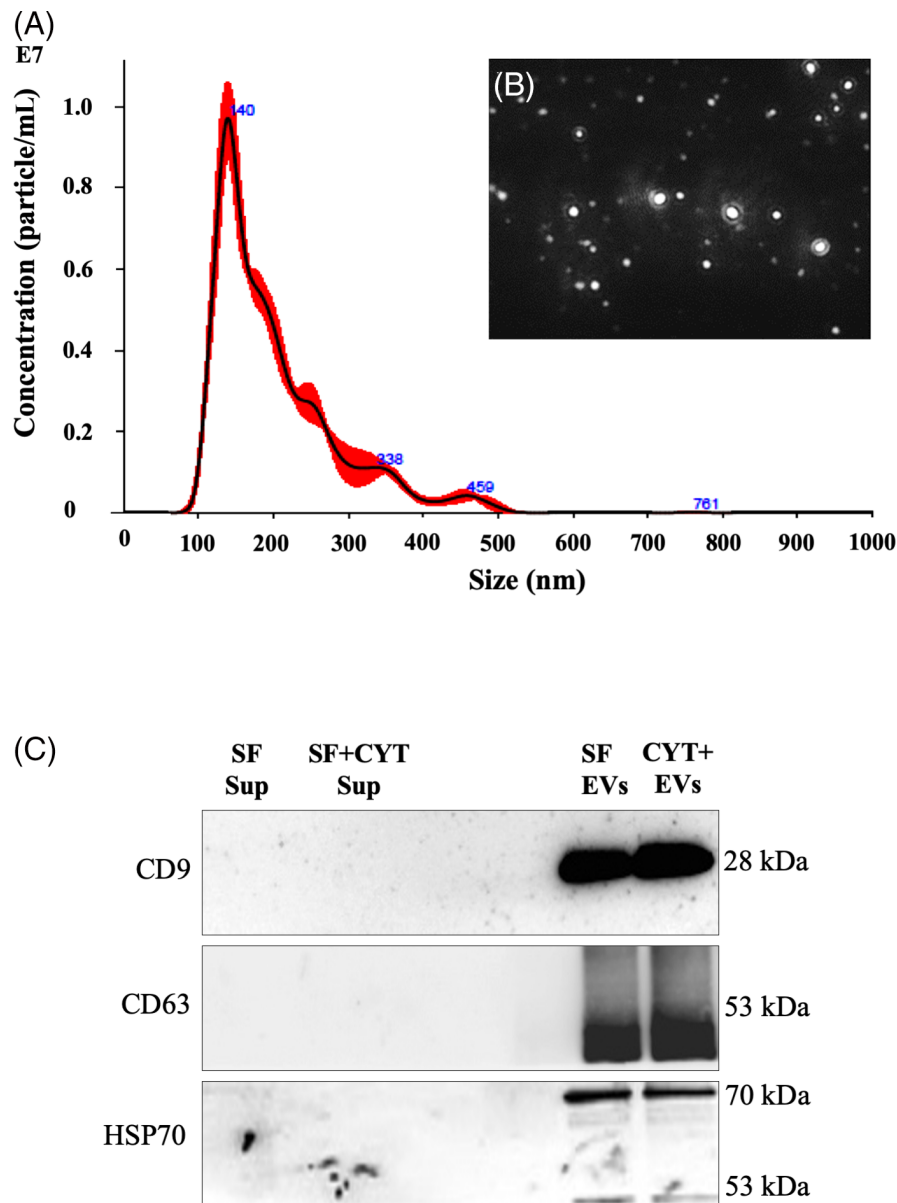

FIGURE 2 pMSC-derived EV characterization. A, Size-distribution curve generated by NS300 NanoSight NTA (data are obtained by mean of three tracking video files, for each experiment): a main pick at a range size of 100 to 500 nm (mean size: 201.1 nm) is visible. B, Frame picture from NTA video, visualizing light scattering EVs derived from cytokine-preconditioned MSCs. Note the presence of vesicles of different sizes. C, EV characterization by WB: the expression of EV markers after serum deprivation (SF) in the presence (CYT+EVs) or in the absence (SF-EVs) of cytokines. EVs were positive for all the three typical markers analyzed. For each lane, 20 μg of proteins derived from the EV pellet or their respective supernatants (SF Sup, SF+CYT Sup.), derived from the last ultracentrifugation before the wash passage (see Section 2) were loaded. EVs, extracellular vesicles; MSCs, mesenchymal stem cells; NTA, nanoparticle tracking analysis; pMSC, preconditioned mesenchymal stem cell; SF, serum-free

then, black signal was inverted for the analysis with Imaris image processing software (Bitplane Software, UK). Dendritic length and the number of spines of neurons were reconstructed by using Autopath system of Imaris (FILAMENT COMMAND) with each single spine detected by the software being manually checked to avoid false positive signals. To reduce the bias related to different dendrite lengths, the medium spine density for each animal was calculated by dividing the total number of spines with the total length of every measured dendrite.[43]

4.7 | Statistical analysis

Comparison between groups of in vitro studies used paired, one-tailed Student's t test. Data are presented as mean ± SEM from at least three independent experiments. Data from in vivo studies are expressed as mean ± SD and groups were compared using the unpaired, two-tailed Student's t test. Differences were considered significant at *P < .05, **P < .01, and ***P < .001.
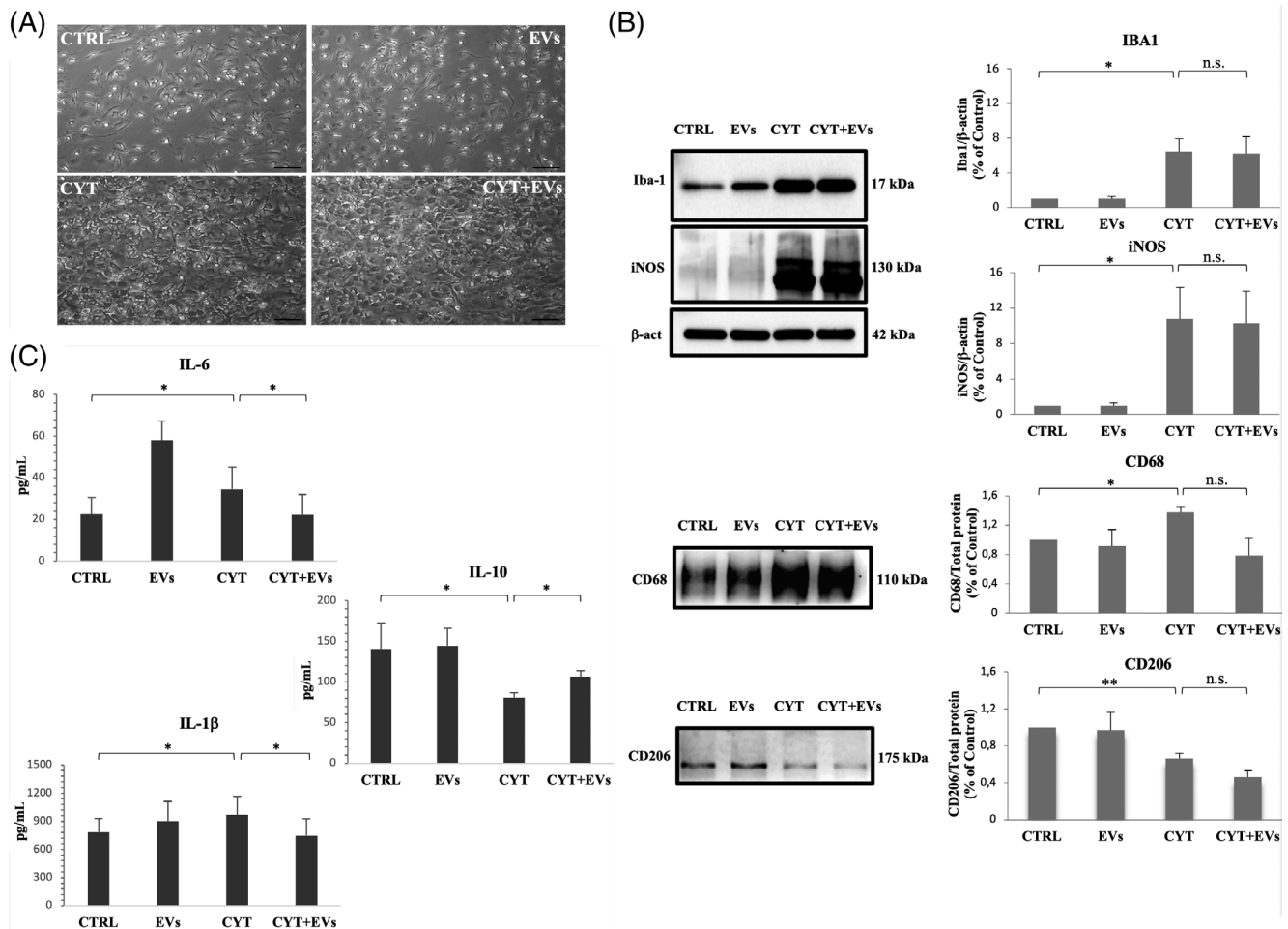

FIGURE 3 EVs switch microglia toward an anti-inflammatory phenotype. A, Cells in control conditions displayed a morphology characterized by thin and long processes (CTRL, EVs). After cytokine treatment, microglia acquire a reactive phenotype defined by bigger soma and amoeboid-like morphology (CYT). The presence of EVs did not alter microglial morphology neither in control (EVs) nor in inflammatory conditions (CYT +EVs). Images were acquired by phase contrast microscopy. Magnification ×10. Scale bars = 100 μm. B, Representative WB bands (left column) and relative quantification histograms (right column) of microglial markers. Cytokine treatment caused a significative upregulation, when compared to the controls, of the activation of M1 markers such as Iba-1, iNOS, and CD68, while downregulated the M2 marker CD206. EV treatment did not significantly affect the expression of none of the markers after the inflammatory challenge (Iba-1, CD68: n = 3; iNOS: n = 4, CD206: n = 4). β-actin was used as loading control for Iba-1 and iNOS expression analysis, while CD68 and CD206 expression was normalized on total protein (Ponceau staining). Comparison between groups (eg, CYT vs CYT+EVs, CTRL vs CYT) used paired, one-tailed Student's t test. C, EV treatment switched microglia toward an anti-inflammatory phenotype. Histograms show the quantification of microglia release of IL-6, IL-1β, and IL-10 by ELISA. In TNFα-IFNγ activated microglia, EVs induced the release of the anti-inflammatory cytokine IL-10 (n = 6) and negatively modulated the secretion of the pro-inflammatory mediators IL-6 (n = 4) and IL-1β (n = 5). (CTRL: control; EVs: extracellular vesicles; CYT: cytokines). For the comparison between groups (eg, CYT vs CYT+EVs, CTRL vs CYT, CTRL vs EVs) paired, one-tailed Student's t test was used; *P < .05, **P < .01. All the data are expressed as ±SEM. ELISA, enzyme-linked immunosorbent assay; EVs, extracellular vesicles; iNOS, inducible nitric oxide synthase

5 | RESULTS

5.1 | Cytokine preconditioning increases MSC immunomodulatory marker expression

After isolation from bone marrow, MSCs were cultured, expanded in vitro, and characterized for their morphology and for marker expression in order to confirm cell phenotype,

according to ISCT minimal definition criteria[44] (Figure S3, see also Reference 35).

Based on the assumption that preconditioning protocols represent key strategies to enhance MSC immunomodulatory functions, we investigated after 24 or 48 hours, the effects of cytokine preconditioning (20 ng/mL TNFα + 25 ng/mL IFNγ) on the expression of the two markers COX-2 and IDO, which are strongly associated to MSC immunocompetence.[45-47]
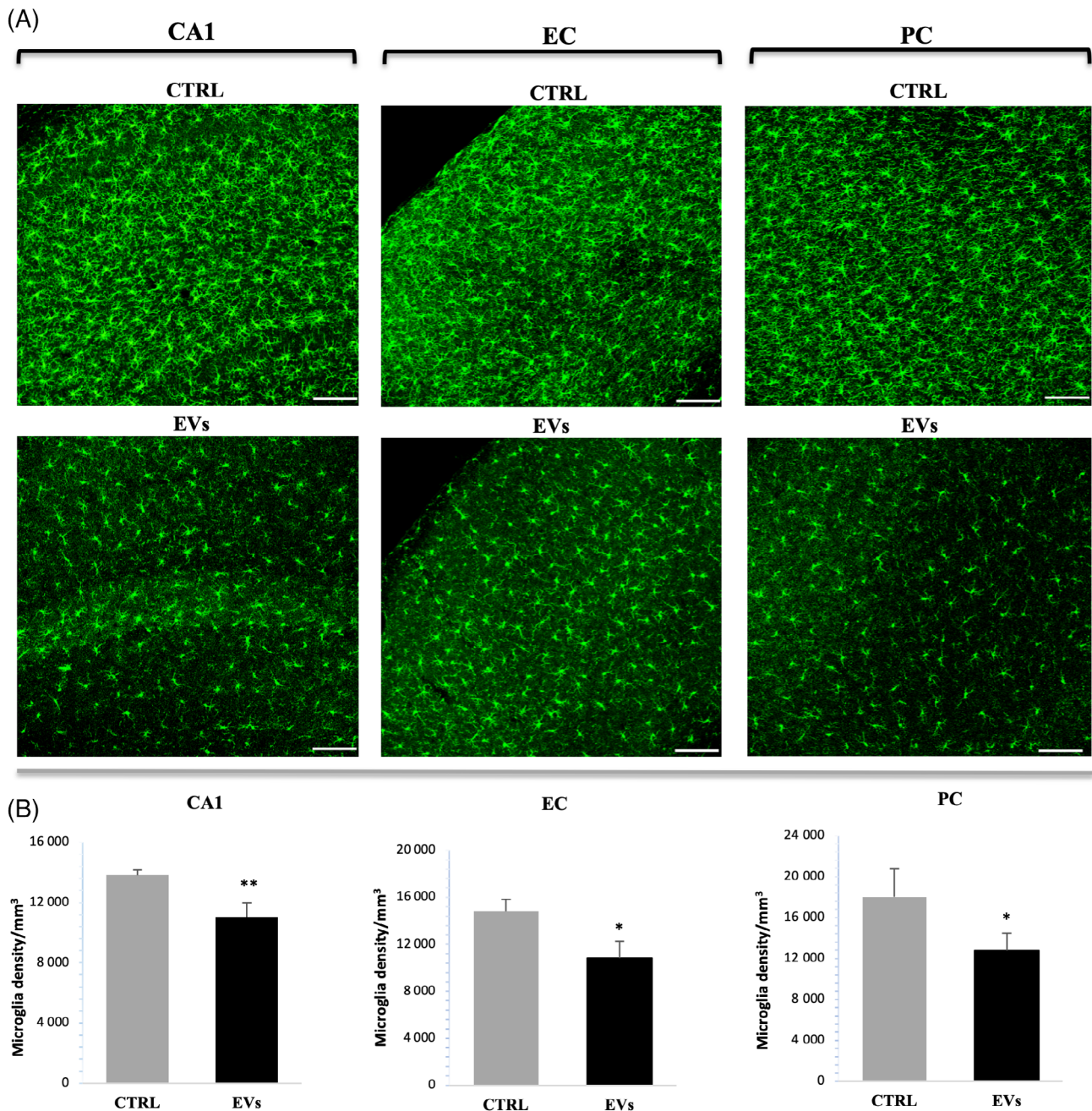

FIGURE 4 IN administration of EVs reduces the density of Iba-1$^+$ cells in 3xTg AD mice. A, Representative images of the distribution of Iba-1$^+$ (green) microglia in the CA1 medial hippocampus (CA1), entorhinal cortex (EC), and prefrontal cortex (PC) of control (CTRL) and EV-treated mice (EVs). B, Histograms compare the number of microglial cells in the same areas of (A). Note that the animals receiving EVs (EVs) displayed a reduced number of Iba-1$^+$ cells compared to animals from the control group that received Phosphate Buffered Saline (PBS). For the comparison between groups (n = 4), unpaired two-tailed Student's t test was used; *P < .05, **P < .01. Data are expressed as arbitrary unit (a.u.) mean ± SD. Scale bars = 100 μm. AD, Alzheimer's disease; EVs, extracellular vesicles

We first tested whether cytokine treatment (SF+CYT) modified the MSC multipotential ability to differentiate in osteocytes and adipocytes (Figure 1A), or changed the expression of the typical CD73 and CD90 stemness markers (Figure 1B). None of these processes were significantly altered, indicating that protocol did not change MSC stemness characteristics. Then the modulation of COX2 and IDO expression, after MSCs underwent to the preconditioning protocol (pMSCs), was investigated (Figure 1B). In the presence of pro-inflammatory cytokines, the immunomodulatory markers were upregulated in a time-dependent manner, with COX2 being mainly induced at 24 hours (Figure 1C; 24 hours: 30.4% vs 48 hours) and IDO at 48 hours (Figure 1C; 48 hours: 168.2% vs 24 hours). Since the overall highest increment (protein expression relative to β-actin expression) of the two markers was observed at 48 hours (Figure 1C), the 48 hours SF+CYT was selected as the MSC stimulation protocol in order to obtain immunocompetent-derived EVs for in vitro and in vivo experiments.

5.2 | Isolation and characterization of pMSC-derived EVs

EVs were isolated from the conditioned medium (CM) of pMSCs and analyzed for protein concentration. The total amount of EVs obtained from $\cong 7 \times 10^6$ cells ranged between 30 and 40 μg corresponding vesicular proteins. NTA allowed the characterization of EVs in suspension: the average size of isolated EVs was 200 nm while the concentration was 1×10^9 particles/mL (Figure 2A,B). To evaluate if the inflammatory challenge could alter the expression pattern of EV typical proteins, we compared, by WB analysis, SF+CYT-EVs and SF-EVs (the latter considered as the control), derived from CM of MSCs maintained in the presence or the absence of cytokines, respectively. No significant difference was observed between the two EV populations, which resulted positive for CD9, CD63, and HSP70 (Figure 2C). Moreover, no signal for the three investigated markers was found in the supernatants of the two EV pools, suggesting an efficiency of the isolation procedure by the ultracentrifugation method. Altogether these results show that the preconditioning protocol does not impact on the quality of the isolation of bona fide pMSC-EVs.

5.3 | pMSC-EVs polarize primary microglia toward an anti-inflammatory phenotype in vitro

To assess their ability to modulate microglia functionality, EVs were administered to primary microglial cultures subjected or not to a pro-inflammatory insult, according to the experimental paradigm depicted in Figure S1. Microglial cells were challenged with TNFα (20 ng/mL) and IFNγ (25 ng/mL) to drive them toward a pro-inflammatory phenotype. Upon treatment, microglial cells switched their morphology characterized by the presence of long and thin processes (*resting* phenotype; Figure 3A, CTRL) to an activated amoeboid (*reactive*) phenotype, showing larger somata and less branched processes (Figure 3A, CYT). The administration of EVs did not influence microglial morphology either in control (Figure 3A, EVs) or in inflammatory conditions (Figure 3A, CYT+EVs).

Then we investigated if EV treatment for 48 hours could modulate the expression of typical microglial markers (Figure 3B). As expected, the exposure to the inflammatory cytokines significantly upregulated
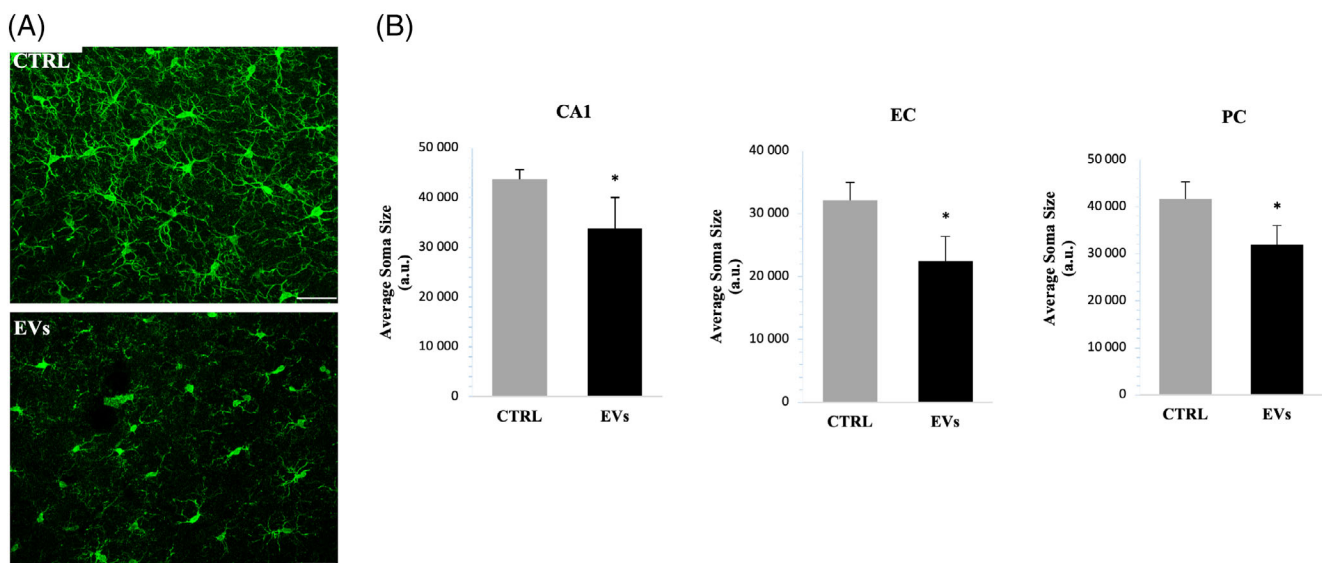

FIGURE 5 IN administration of EVs reduces cell soma size of Iba-1^{+} cells. A, Representative image of microglia cells stained for Iba-1 in medial hippocampus CA1 of control (CTRL) and EV-treated (EVs) 3xTg AD mice. Scale bars = 30 μm. B, Histograms comparing the reduction (shown as a.u.) of microglial cell body size in hippocampus (CA1), entorhinal cortex (EC), prefrontal cortex (PC) of control and treated mice. Average cell body size was quantified by means of ImageJ software (see the thresholding method description in Supporting Information). Comparison between groups (n = 4) used unpaired, two-tailed Student's *t* test; *P < .05. Data are expressed as mean ± SD. EVs, extracellular vesicles

the expression of Iba-1 (+545.1% vs CTRL), an actin-binding protein normally increased after cell activation.[48] Moreover, activated microglia underwent upregulation of common pro-inflammatory markers such as the inducible nitric oxide synthase (iNOS) (+975.3%) and the lysosomal phagocytic protein CD68 (+37.3%), while the typical anti-inflammatory marker CD206, the mannose receptor with a repair function, was significantly downregulated (−33.7%).

Albeit unable to revert the expression of microglial markers (Figure 3B, CYT+EVs), EVs significantly affected microglial function (Figure 3C). In fact, cytokine treatment increased, as expected, microglial release of the pro-inflammatory mediators IL-6 (CTRL: 22.54 ± 8.06 pg/mL; CYT: 34.60 ± 10.60 pg/mL) and IL-1β (CTRL: 784 ± 148.70 pg/mL; CYT: 970 ± 194.31 pg/mL), while it downregulated the production of the anti-inflammatory cytokine IL-10 (CTRL: 140.65 ± 31.93 pg/mL; CYT:
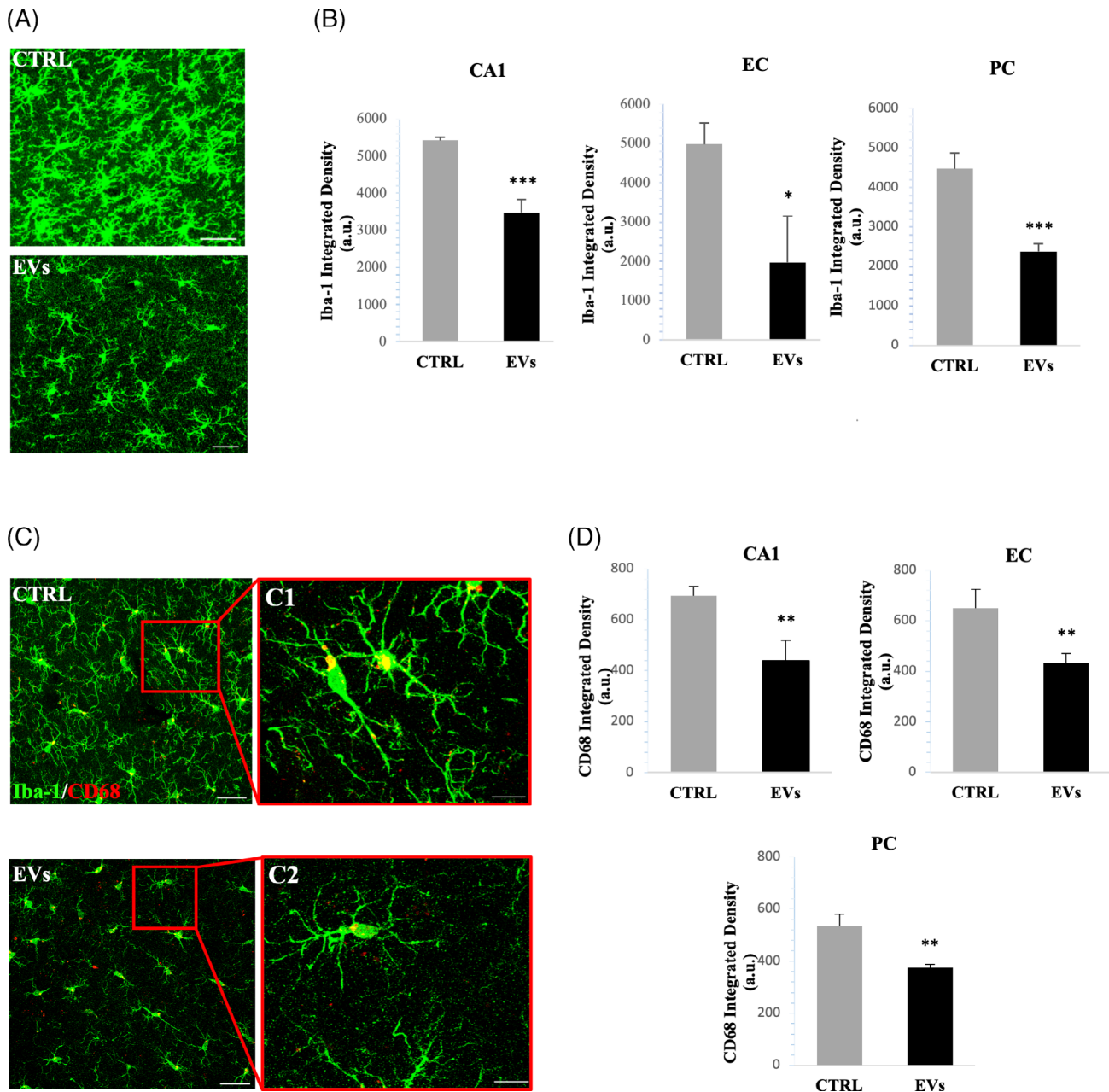

FIGURE 6 pMSC-derived EVs reduce Iba-1 and CD68 expression in microglia of AD mice. A,C, Representative confocal images of the hippocampal CA1 region showing the effect of EVs in lowering the expression of Iba-1 (A, green) and CD68 (C, red) in microglial cells of EV-treated (EVs) compared to control mice. Scale bars (A, C) = 30 μm; C1 and 2: magnified views of the boxed regions in (C) = 10 μm. Note in C1 and C2, the yellow/orange dots representing CD68 and Iba-1 colocalization. B,D, Histograms comparing the quantification of the fluorescence intensity of Iba-1 (B, n = 4) and CD68 (D, n = 4) in CA1 region of the medial hippocampus (CA1), entorhinal cortex (EC), and prefrontal cortex (PC) of control (CTRL) and EV-treated mice (EVs). Comparison between untreated and treated groups (CTRL vs EVs) used unpaired, two-tailed Student's t test; *P < .05, **P < .01, and ***P < .001. Data are expressed as mean ± SD. AD, Alzheimer's disease; EVs, extracellular vesicles; pMSCs, preconditioned mesenchymal stem cells

80.90 ± 6.05 pg/mL). Noteworthy, EV administration to microglia significantly reduced the secretion of IL-6 (CYT: 34.60 ± 10.60 pg/mL; CYT +EVs: 22.37 ± 9.60 pg/mL) and IL-1β (CYT: 970 ± 194.31 pg/mL; CYT +EVs: 746 ± 179.13 pg/mL). In addition, EVs reverted the inhibitory effect of TNFα and IFNγ on IL-10, by restoring cytokine release to almost control levels (Figure 3C; CYT: 80.9 ± 6.05 pg/mL; CYT+EVs: 106.43 ± 7.49 pg/mL). IL-4, a prototypical anti-inflammatory cytokine typically associated with repair/regenerative polarization of microglia, was not detectable in our experimental settings (not shown).

5.4 | MSC-EVs decrease microglia activation in 3xTg AD mice

For the in vivo studies, we used 3xTg AD mice (see experimental design in Figure S2), focusing our attention on the hippocampus, entorhinal, and prefrontal cortices, since these regions show a different microglial activation at 7 months of age.[49] Before evaluating the immunoregulatory potential of EVs in 3xTg mice, we qualitatively investigated whether intranasal (IN) administration of
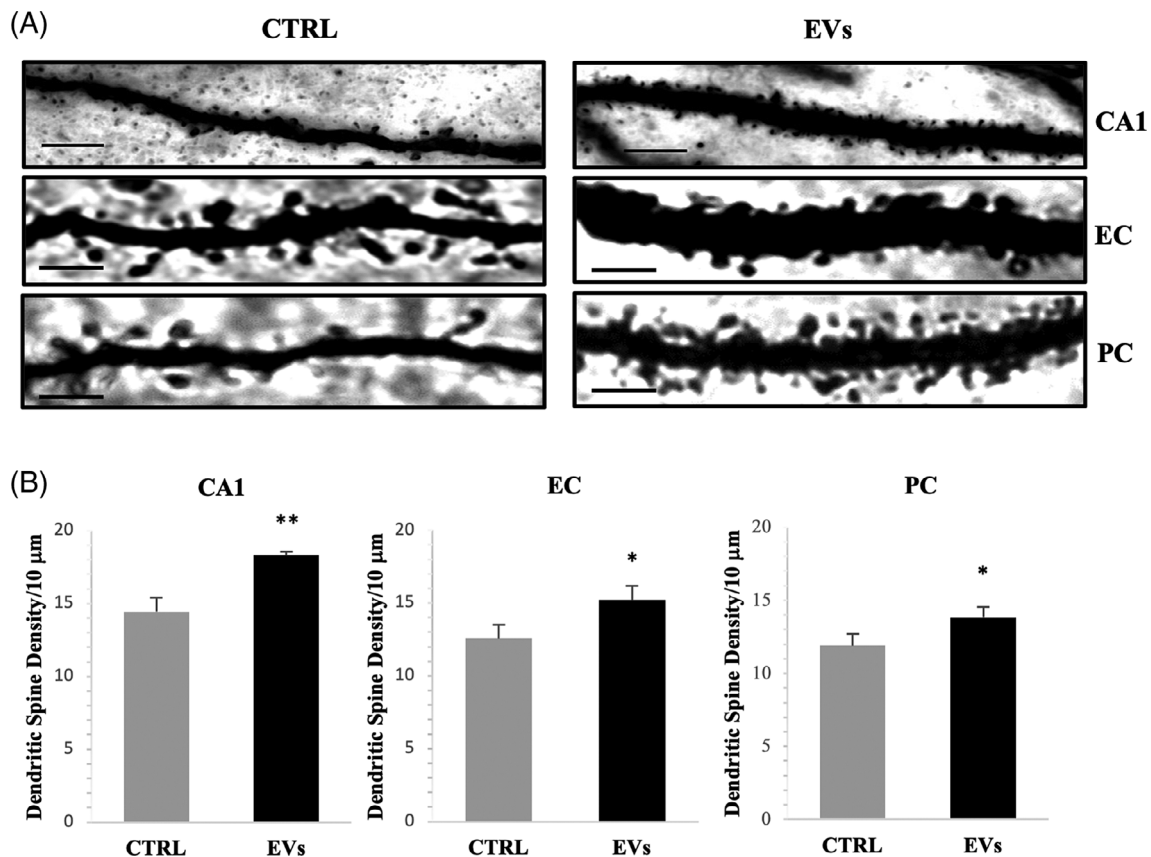

FIGURE 7 MSC-derived EVs increase dendritic spine density in 3xTg mice. A, Representative photomicrographs of Golgi-Cox stained dendritic segments from hippocampal CA1 pyramidal neuron (CA1), entorhinal cortex (EC), and prefrontal cortex (PC) neurons, of control (CTRL) and EV-treated mice (EVs). Scale bars = 5 μm. B, Histograms show the quantification of dendritic spine density (spines/10 μm) in the same areas. Animals treated with EVs (EVs) display a significative higher number of dendritic spines compared to the nontreated group (CTRL). *P < .05; **P < .01. EVs, extracellular vesicles; MSCs, mesenchymal stem cells

TABLE 1 The numeric values corresponding to the total number of counted dendritic spines and the total length of dendritic processes that were considered for the analysis of the mean dendritic spine density per 10 μm dendritic length (mean density/10 μm)

Group	CA1		EC		PC	
	CTRL	EVs	CTRL	EVs	CTRL	EVs
Mice (no.)	4	4	4	4	4	3
Dendritic length (μm)	1882.37	1698.94	1716.38	1029.77	669.17	695.52
Dendritic spines (no.)	2735	3099	2181	1562	794	956
Mean density/10 μm	14.44	18.30	12.58	15.20	11.89	13.80

Note: Comparison between untreated and treated groups (CTRL vs EVs) used unpaired, two-tailed Student's t test. Data are expressed as mean ± SD.

Abbreviations: EC, entorhinal cortex; EVs, extracellular vesicles; PC, prefrontal cortex.

PKH26-labeled EVs could result in the delivery of the vesicles into the aforementioned brain areas. Within 6 hours from EV treatment, labeled MSC-EVs were robustly incorporated into CA1 microglia (Figure S4A,A1) and, to some extent, into neurons (Figure S4B,B1), but not in astrocytes (Figure S4C,C1). This pattern of internalization was observed also in the other investigated regions (not shown).[50]

Once assessed that EVs properly target the brain, we evaluated their effects on microglia activation. We first focused on the number of microglia cells, as their proliferation is one of the typical signs of cell activation.[51] By Iba-1 antibody IF staining of brain coronal sections of 3xTg mice receiving PBS (referred to as control, CTRL) or EVs (Figure 4A), we observed that EV-treated mice displayed a strong decrease of Iba-1^{+} cell density compared to CTRL in all analyzed regions (Figure 4B; hippocampus: −20.14%; entorhinal cortex: −27.16%; prefrontal cortex: −29.17%).

Since cell soma hypertrophy is a typical morphological feature of reactive microglia,[52] we also measured microglial cell body size in EV-treated (EVs) and CTRL groups (Figure 5A). The administration of EVs induced a reduction of the average cell body size in all the analyzed regions (Figure 5B; hippocampus: −22.76%; entorhinal cortex: −30.12%; prefrontal-cortex: −23.37%).

In order to further characterize the activation state of microglia cells, we analyzed the fluorescence intensity of Iba-1 (Figure 6A), whose expression is enhanced by cell activation.[48] The quantitative analysis of the fluorescence integrated density indicated that EV administration strongly reduce Iba-1 expression compared to CTRL (Figure 6B; hippocampus: −35.86%; entorhinal cortex: −60.44%; prefrontal cortex: −46.79%). We then examined the expression of CD68 (Figure 6C) and CD206 markers associated to the activated and deactivated phenotypes, respectively. The quantitative analysis showed that EV treatment significantly reduce CD68 expression (Figure 6D; hippocampus: −36.89%; entorhinal cortex: −33.13%; prefrontal cortex: −29.76%). No significant difference between the two groups was detected for CD206 (Figure S5). Overall, these results suggest that MSC-EVs exert a dampening effect on polarization of microglia toward a pro-inflammatory phenotype.

5.5 | MSC-EVs increase dendritic spine density in 3xTg mice

Since reactive microglia has been demonstrated to actively mediate synapse loss in AD,[53,54] we wondered whether EV-induced modulation of microglia phenotype correlated with a neuroprotective profile. To investigate this point, we focused on the analysis of the dendritic spine density (Figure 7). Golgi-Cox staining of brain tissues (Figure 7A and Table 1) revealed that IN-injected EVs increase spine density, compared to CTRL group animals (Figure 7B; hippocampus: +26.72%; entorhinal cortex: +20.83%; prefrontal cortex: +16.08%). In the attempt to define whether MSC-EVs could exert a direct effect on neuronal cells, we set up 3xTg neuronal primary cultures and treated

with cytokines following the experimental paradigm used as for microglial cells (Figure S6). In our experimental conditions, none significative difference in synaptophysin expression was detected in EV-treated and not-treated neurons after the inflammatory challenge. Moreover, cell vitality and morphology were not affected by both cytokine and EV treatments.

6 | DISCUSSION

The discovery that MSC-derived EVs mediate immunomodulatory effects similarly to the cells of origin (for a review, see Reference 55) has paved the way for the study of their contributions in tissue and organ repair.

Here, we assessed the effects of MSC-EV anti-inflammatory properties in in vitro and in vivo preclinical models. We isolated highly immunocompetent EVs, by preconditioning MSCs (pMSC) with TNFα and INFγ for 48 hours, inducing the upregulation of COX2 and IDO, which associate to a MSC immunoregulatory polarized phenotype.[45-47] COX2 upregulation is usually linked to Prostaglandin E2 (PGE2) increase. Interestingly, PGE2 was found to be constitutively produced by human MSCs at levels able to suppress IL-6 and TNF-α expression in activated macrophages.[56]

The EV anti-inflammatory effects were demonstrated in an in vitro model of inflammation, consisting of primary cultures of microglia cells subjected to a pro-inflammatory insult. MSC-EVs reduced the secretion of IL-6 and IL-1β, which play important roles in neuroinflammation and which are upregulated in AD brains,[57,58] while enhancing the secretion of IL-10—a potent anti-inflammatory cytokine which induces the M2c polarization state (the "deactivated" phenotype)—associated with the formation of neuronal synapses.[59] A similar result has been described by Lo Sicco et al who elicited the switch of macrophages from M1 to M2 phenotype, upon their exposure to EVs of human adipose cells exposed to normoxic or hypoxic conditions.[23] These data suggest that MSC-EVs can drive a functional polarization of microglia toward an anti-inflammatory phenotype in vitro and are in line with previous in vitro evidence showing that MSC-EVs are able to limit the inflammatory response by preventing the production of pro-inflammatory molecules by microglia/macrophages.[60,61]

In spite of the positive results on microglial functionality, the treatment with pMSC-EVs did not affect either cell morphology, or the expression of Iba-1, usually upregulated after microglial activation.[62] In addition, CD68, iNOS, considered as pro-inflammatory markers, and CD206, the mannose receptor widely recognized as a typical protective factor with important functions in pinocytosis and phagocytosis,[63,64] were not modulated by EV treatment in vitro. A correlation between functional (ie, the modulation of the release of cytokines) vs phenotypic parameters (ie, the lack of changes in the expression of pro- or anti-inflammatory markers) would have been expected. We can presume that the difference that we observed may reflect the diverse temporal window needed for EV modulation in vitro. To our knowledge, the studies demonstrating a correlation between the release of cytokines and marker expression (see for

instance, References 18 and 65) focused on the quantification of cytokine gene expression (RNA), rather than protein levels released in the extracellular medium. Hammond et al[66] recently reported that microglia exist in multiple definable states that change during development, aging, and injury. These distinct microglia subpopulations are characterized by different transcriptional signatures, reflecting a specific and definable transcriptional program. Interestingly, according to Hammond et al, the highest microglial diversity is detectable at the early development, when microglia are still differentiating.[67] Since we performed the in vitro experiments on microglia isolated from newborn mice, the possibility that our results could somehow underlie the microglia variability occurring at young age is a tantalizing hypothesis.

Of note, the anti-inflammatory EV modulation of cytokine release was observed when microglial cells were in the presence of the inflammatory insult (Figure 3, "CYT+EVs"). Interestingly, MSC ability to modulate immune responses has been proposed to rely, at least in part, on the activation of two "negative feedback loops" (the PGE2 and TSG-6 feedback loops).[68] According to the "loop hypothesis," MSCs could switch-off inflammation by activating one loop or the other, depending on the environmental conditions, to drive resident macrophages toward an anti-inflammatory phenotype, only when inflammatory responses are switched on. It is reasonable to assume therefore that also EVs, inheriting MSC features, could exert their anti-inflammatory effects only on TNFα-INFγ-polarized microglia, when inflammatory pathways have been activated. However, the unexpected increase of IL-6 release from control microglia (Figure 3C, "EVs") is puzzling and will need further investigation. It has to be considered though that IL-6 plays pleiotropic roles, through the activation of the STAT3 pathway, not only in pathological conditions. Indeed, Kushima and Oh demonstrated IL-6 ability to act in a trophic manner and promote neuronal differentiation.[69,70] If these pleiotropic actions could be activated also in our cultures is still something to explore.

Similarly, also IL-1β was negatively affected by MSC-EVs after the inflammatory challenge. However, as well as IL-6, IL-1β secretion appeared positively modulated in control microglial conditions, albeit with a lesser extent than IL-6 and in a not statistically significant manner. Interestingly, Sato et al[71] demonstrated that in microglia/macrophages IL-1β was able to increase the expression of alternative activation markers such as Ym1 and arginase-1 and suppress spinal cord injury by the reduction of the inflammatory responses. These data may suggest a role of IL-1β in fostering brain repair, other than being involved in the inflammatory cascade. Thus, the pro-inflammatory and anti-inflammatory properties of both IL-6 and IL-1β—that reflect the dynamism of the inflammatory process—appear to be strictly context-dependent and may provide the explanation for the different modulation observed in control and TNFα-INFγ-challenged microglia after EV treatment. Possibly, also IL-4 or IL-10, typically considered as anti-inflammatory cytokines, may display a pro-inflammatory function based on the different contexts and environments.[72] This would certainly need to be taken into account in light of possible therapeutic application of any tool (cells or EVs) affecting cytokine release.

Regarding the trend of increase of IL-6 and IL-1β in control conditions, we cannot exclude a direct delivery of the cytokines by EVs, although this possibility could also occur under stimulated conditions. In line with this assumption, interestingly, it has been recently reported that bioactive cytokines might be released in a EV-encapsulated form.[73] The pattern of EV-encapsulation seems to be strictly dependent on the environmental stimulus, suggesting that the sorting of cytokines in EVs relies on a highly regulated biological process that can drive the release of that cytokine predominantly in the soluble form and/or in association to EVs (encapsulated- or surface-bound form). Even though the biological meaning of loading cytokines into EVs still needs to be clarified, the authors speculate that cytokine release in the free form or associated with EVs could depend on specific physiological requirements, in particular if these cytokines need to play their functions in proximity of the secreting cell (as soluble) or at a distance (as EV-encapsulated[73]). Although some cytokines seem to be preferentially released in EVs and others in the free form, it appears that any given cytokine can be encapsulated into EVs, including IL-10, IL-4, IL-6, and IL-1β. Therefore, we cannot rule out the possibility that also in our experimental system, EV-encapsulated cytokines could be present, since, by ELISA, we were able to detect only soluble ones.

Both functional and proteomic analysis of EVs derived from preconditioned compared to not-preconditioned MSCs would help to clarify the mechanism underlying the different microglia response to EVs after an inflammatory insult or in control conditions.

One of the major contributions of our study is that we used the intranasal (IN) route to administer MSC-EVs in 3xTg mice, enabling the modulation of microglia phenotype and dendritic spine integrity. As far as we know, this is the first time that MSC-EVs have been delivered via IN route in an AD model. MSCs, as whole cells, have been tested for their therapeutic ability in AD in different preclinical models. In particular, transplantation of MSCs in AD mice has been associated to: (a) inhibition of Aβ- and tau-related cell death[74,75]; (b) reduction of Aβ deposits and plaque formation[76-80]; (c) stimulation of neurogenesis, synaptogenesis, and neuronal differentiation[74,77]; (d) ability to rescue spatial learning and memory deficits.[75,76] Several advantages emerge when using EVs with respect to the whole cells, among which EVs are safer and easier to handle due to their smaller size and the absence of the nucleus, thus avoiding self-replication, and highly reducing the cell endogenous tumorigenic potential. Moreover, EVs, as carriers for bioactive molecules, may be exploited for overcoming tissue barriers to reach specific cell populations.[81]

IN administration of EVs has been tested in neurological disorders including Parkinson's disease[82] and status epilepticus (SE), both in pilocarpine-induced[50] or kainate-induced[83] models of SE, lipopolysaccharide (LPS)-induced brain inflammation model, experimental autoimmune encephalomyelitis, GL26 tumor model,[84] and the autism BTBR T+tf/J (BTBR) mice model.[85] However, except for the LPS-acute inflammatory model,[84] all these studies have exploited chronic EV treatment, with mice being sacrificed at the end of the treatment. In our study, instead, mice were sacrificed 3 weeks after only two IN injections—at close interval of time—with MSC-derived EVs, allowing

us to ascertain their *long-lasting* anti-inflammatory and neuro-protective effects and paving the way for a less invasive and more translational use of these biological round lipid bilayers in AD.

The neuroprotective effects of EVs from MSCs in AD have already been proposed by few studies performed in APP/PS1 mice.[32,33] Canales-Aguirre's group[86] tested MSC-EVs effects on an acute model of AD showing that MSC-derived exosomes promote neurogenesis and cognitive functional recovery. None of these studies, however, delivered MSC-EVs intranasally.

The in vivo analysis of the immunomodulatory potential of MSC-EVs was focused on microglial activation. At this aim, we used 7-month-old 3xTg mice since, at this age, virtually no Aβ plaques and neurofibrillary tangles (NFTs)[87] are displayed, but typical traits of microglial activation are already present.[49,88,89] The increase of microglia number is typically observed in postmortem AD brains[90] and in AD preclinical models.[88,89,91] In our study, the presence of EVs was linked to a strong reduction of the number of Iba-1-positive cells in all the analyzed regions of treated group after 3 weeks. This might outcome in a relevant therapeutic value, since strategies affecting the expansion of microglial cells brought beneficial consequences in AD mice.[92,93] In addition, one of the criteria to morphometrically characterize "primed" vs "reactive" microglia is the hypertrophy of the cell soma.[52] Noteworthy, EV treatment caused a significative decrease of microglia soma size. Moreover, it reduced the expression of Iba-1 and the lysosomal marker CD68, while no change in CD206 expression was observed.

Iba-1 staining was used to identify the activated microglia (Figures 4-6), although it may also have detected some local or infiltrating Iba-1$^+$ macrophages.[94,95] Noteworthy, an immunomodulatory effect of MSC-EVs on macrophages has been described by Agudelo et al.[96] Along with microglia and macrophages, a certain amount of other cells derived from blood can contribute to the inflammatory response that characterizes the AD brains. In fact, neutrophils, T cells, and B cells could cross the damaged blood brain barrier (see, eg, Reference 97), thus contributing to the exacerbation of central inflammation. Indeed, activation of circulating peripheral immune cells is observed in patients with early stages of AD.[98-100] The possible action of MSC-EVs also on peripheral infiltrates will deserve to be considered in future studies.

Altogether these results indicate an EV dampening action on microglia activation that may lead to a functional switch of microglia toward a less phagocytic cell population. Such a functional switch recalls data achieved in a mice model of traumatic brain injury in which the authors demonstrated a downregulation of CD68 expression following ICV injection of MSCs.[101] Unexpectedly, our in vitro data, showing no modulation of CD68 expression, do not seem to match with the in vivo ones. It can be hypothesized that this discrepancy could reflect an unbridgeable difference of the time window analysis (few days vs few weeks). Furthermore, it should be taken into account a possible indirect role of neurons or other glial cells in modifying the expression of the phagocytic marker in vivo; something that cannot be guaranteed in our experimental model in vitro. Remarkably, a direct effect of MSC-EVs has been described in primary

hippocampal cultures that turned out to be protected from oxidative stress and synapse damage induced by amyloid-β oligomers.[102,103] However, our experiments on 3xTg hippocampal neurons (Figure S6) seem to rule out, at least in our experimental settings, a direct effect on neuronal activity. We are aware of all the limitations of an in vitro system and believe that this question still remains open and certainly deserves further investigations in order to ascertain or exclude a direct action in vivo.

Since hyperactivated microglia may dramatically contribute to synapse loss in AD[54] and early microglia proliferation has been demonstrated in 3xTg mice in a plaque-free stage,[88] we wondered whether EV effects on microglia cell activation could somehow result in a protective effect on neurons. Intriguingly, EV-treated group displayed a significative increment in the dendritic spine density in all the evaluated regions. Although a direct correlation cannot be established yet, we can speculate that the increase in dendritic spines may correlate to the EV immunomodulatory effects. This could imply that EVs might counteract the degeneration of dendritic spines by reducing inflammatory mediators that contribute to neuronal damage.[104] In support of this view is the study by Tong et al who demonstrated, in organotypic hippocampal slices, that IL-1β was able to inhibit BDNF-dependent long term potentiation (LTP) and dendritic spinogenesis in hippocampal slices.[105] Conversely, the application of IL-10 to hippocampal neurons in vitro induced neuronal synapse formation and increased dendritic spine density.[59]

Microglia have been suggested to phagocytose synapses under pathological conditions[53,54] exerting detrimental effects that contribute to the disease pathogenesis. Microglia-mediated synapse loss seems to involve an increased expression of the lysosomal protein CD68, that, in the hippocampus of J20 AD mice, colocalizes with engulfed synaptic proteins,[106] through an internalization mechanism similar to synaptic pruning occurring in the developmental brain. In our study, the treatment with EVs decreased CD68 expression. Therefore, we may hypothesize that a reduction in microglia phagocytic activity could represent another mechanism underlying the increase of dendritic spine density observed after EV treatment.

7 | CONCLUSIONS

Recent studies, including ours showing a potential role for MSC-EVs already in the early stages of AD,[34] sustain the use of MSC-EVs to exert beneficial effects in animal models of AD through the regulation of the inflammatory and oxidative processes.[32,33] However, in these studies, EV administration was performed intravenously or intracerebroventricularly for weeks or months in APP/PS1 AD mice. We believe that the striking aspect of our study resides in that the observed effects on microglia activation and dendritic spines were achieved by only two temporally close IN injections of MSC-EVs. This could possibly occur because EVs delivered upon this administration route could reach higher levels than those delivered by others.[107] Undoubtedly, the possibility of obtaining greater effects by repeated

IN injections has to be considered and will be matter of future experiments.

In conclusion, our results strengthen the view that mechanisms of action other than removal of amyloid plaques from the brain should deserve a great attention when treating AD. Likewise, the promising effects induced by MSC-EVs support the IN delivery of MSC-EVs, being safe and low invasive, as a possible approach for a therapeutic intervention in AD, at least so far in preclinical models.

ACKNOWLEDGMENTS

CONFLICT OF INTEREST

The authors declared no potential conflicts of interest.

AUTHOR CONTRIBUTIONS

M.L.: conception and design, collection and assembly of data, data analysis and interpretation, manuscript writing; M.P. (in vivo experiments): conception and design, collection of data, data analysis and interpretation; C.D., L.R., L.M., E.B. (in vitro experiments): collection of data; C.A.E.: provision of study material; F.M. (in vitro experiments): collection and assembly of data, data analysis; E.L., A.B. (in vitro experiments): data analysis and interpretation; M. Mauri (in vivo experiments): data analysis and interpretation; E.D., G.D.: provision of study material (hMSC); A.T.: financial support; M. Matteoli, M.B.: financial support, data analysis and interpretation, final approval of manuscript; S.C.: conception and design, financial support, assembly of data, data analysis and interpretation, manuscript writing, final approval of manuscript.

DATA AVAILABILITY STATEMENT

The data that support the findings of this study are available on request from the corresponding author.

ORCID

Mario Buffelli https://orcid.org/0000-0002-3709-013X

Silvia Coco https://orcid.org/0000-0002-3883-9472

REFERENCES

1. Hardy J, Selkoe DJ. The amyloid hypothesis of Alzheimer's disease: progress and problems on the road to therapeutics. *Science*. 2002; 297:353-356.
2. Kettenmann H, Hanisch U-K, Noda M, Verkhratsky A. Physiology of microglia. *Physiol Rev*. 2011;91:461-553.
3. Limatola C, Ransohoff RM. Modulating neurotoxicity through CX3CL1/CX3CR1 signaling. *Front Cell Neurosci*. 2014;8:1-8.
4. Parkhurst CN, Yang G, Ninan I, et al. Microglia promote learning-dependent synapse formation through brain-derived neurotrophic factor. *Cell*. 2013;155:1596-1609.
5. Shechter R, Schwartz M. Harnessing monocyte-derived macrophages to control central nervous system pathologies: no longer 'if' but 'how'. *J Pathol*. 2013;229:332-346.
6. Kigerl KA, Gensel JC, Ankeny DP, Alexander JK, Donnelly DJ, Popovich PG. Identification of two distinct macrophage subsets with divergent effects causing either neurotoxicity or regeneration in the injured mouse spinal cord. *J Neurosci*. 2009;29:13435-13444.
7. Leyns CEG, Holtzman DM. Glial contributions to neurodegeneration in tauopathies. *Mol Neurodegener*. 2017;12:50.
8. Spangenberg EE, Green KN. Inflammation in Alzheimer's disease: lessons learned from microglia-depletion models. *Brain Behav Immun*. 2017;61:1-11.
9. Czeh M, Gressens P, Kaindl AM. The yin and yang of microglia. *Dev Neurosci*. 2011;33:199-209.
10. Heppner FL, Ransohoff RM, Becher B. Immune attack: the role of inflammation in Alzheimer disease. *Nat Rev Neurosci*. 2015;16: 358-372.
11. Colonna M, Butovsky O. Microglia function in the central nervous system during health and neurodegeneration. *Annu Rev Immunol*. 2017;35:441-468.
12. Hansen DV, Hanson JE, Sheng M. Microglia in Alzheimer's disease. *J Cell Biol*. 2018;217:459-472.
13. Hammond TR, Marsh SE, Stevens B. Immune signaling in neurodegeneration. *Immunity*. 2019;50:955-974.
14. Zhang J, Li Y, Lu M, et al. Bone marrow stromal cells reduce axonal loss in experimental autoimmune encephalomyelitis mice. *J Neurosci Res*. 2006;84:587-595.
15. Lee HJ, Lee JK, Lee H, et al. The therapeutic potential of human umbilical cord blood-derived mesenchymal stem cells in Alzheimer's disease. *Neurosci Lett*. 2010;481:30-35.
16. Cova L, Armentero M-T, Zennaro E, et al. Multiple neurogenic and neurorescue effects of human mesenchymal stem cell after transplantation in an experimental model of Parkinson's disease. *Brain Res*. 2010;1311:12-27.
17. Bao X, Wei J, Feng M, et al. Transplantation of human bone marrow-derived mesenchymal stem cells promotes behavioral recovery and endogenous neurogenesis after cerebral ischemia in rats. *Brain Res*. 2011;1367:103-113.
18. Yokokawa K, Iwahara N, Hisahara S, et al. Transplantation of mesenchymal stem cells improves amyloid-β pathology by modifying microglial function and suppressing oxidative stress. *J Alzheimers Dis*. 2019;72:867-884.
19. Liang X, Ding Y, Zhang Y, Tse HF, Lian Q. Paracrine mechanisms of mesenchymal stem cell-based therapy: current status and perspectives. *Cell Transplant*. 2014;23:1045-1059.
20. Baek G, Choi H, Kim Y, et al. Mesenchymal stem cell-derived extracellular vesicles as therapeutics and as a drug delivery platform. *Stem Cells Translational Medicine*. 2019;8(9):880-886.
21. EL Andaloussi S, Mäger I, Breakefield XO, et al. Extracellular vesicles: biology and emerging therapeutic opportunities. *Nat Rev Drug Discov*. 2013;12:347-357.
22. Stahl PD, Raposo G. Extracellular vesicles: exosomes and microvesicles, integrators of homeostasis. *Phys Ther*. 2019;34: 169-177.
23. Lo Sicco C, Reverberi D, Balbi C, et al. Mesenchymal stem cell-derived extracellular vesicles as mediators of anti-inflammatory effects: endorsement of macrophage polarization. *Stem Cells Translational Medicine*. 2017;6:1018-1028.
24. Álvarez V, Sánchez-Margallo FM, Macías-García B, et al. The immunomodulatory activity of extracellular vesicles derived from endometrial mesenchymal stem cells on CD4+ T cells is partially mediated by TGFbeta. *J Tissue Eng Regen Med*. 2018;12:2088-2098.
25. Elia CA, Losurdo M, Malosio ML, Coco S. Extracellular vesicles from mesenchymal stem cells exert pleiotropic effects on amyloid-β,

inflammation, and regeneration: a spark of hope for Alzheimer's disease from tiny structures? *Bioessays*. 2019;41:1800199.

26. Del Fattore A, Luciano R, Saracino R, et al. Differential effects of extracellular vesicles secreted by mesenchymal stem cells from different sources on glioblastoma cells. *Expert Opin Biol Ther*. 2015;15: 495-504.

27. Cuerquis J, Romieu-Mourez R, François M, et al. Human mesenchymal stromal cells transiently increase cytokine production by activated T cells before suppressing T-cell proliferation: effect of interferon-γ and tumor necrosis factor-α stimulation. *Cytotherapy*. 2014;16:191-202.

28. Saparov A, Ogay V, Nurgozhin T, Jumabay M, Chen WCW. Preconditioning of human mesenchymal stem cells to enhance their regulation of the immune response. *Stem Cells Int*. 2016;2016:1-10.

29. Fatima F, Ekstrom K, Nazarenko I, et al. Non-coding RNAs in mesenchymal stem cell-derived extracellular vesicles: deciphering regulatory roles in stem cell potency, inflammatory resolve, and tissue regeneration. *Front Genet*. 2017;8:161.

30. Hu C, Li L. Preconditioning influences mesenchymal stem cell properties in vitro and in vivo. *J Cell Mol Med*. 2018;22:1428-1442.

31. Ruppert KA, Nguyen TT, Prabhakara KS, et al. Human mesenchymal stromal cell-derived extracellular vesicles modify microglial response and improve clinical outcomes in experimental spinal cord injury. *Sci Rep*. 2018;8:480.

32. Cui GH, Wu J, Mou FF, et al. Exosomes derived from hypoxia-preconditioned mesenchymal stromal cells ameliorate cognitive decline by rescuing synaptic dysfunction and regulating inflammatory responses in APP/PS1 mice. *FASEB J*. 2018;32:654-668.

33. Wang SS, Jia J, Wang Z. Mesenchymal stem cell-derived extracellular vesicles suppresses iNOS expression and ameliorates neural impairment in Alzheimer's disease mice. *J Alzheimers Dis*. 2018;61: 1005-1013.

34. Elia CA, Tamborini M, Rasile M, et al. Intracerebral injection of extracellular vesicles from mesenchymal stem cells exerts reduced Aβ plaque burden in early stages of a preclinical model of Alzheimer's disease. *Cells*. 2019;8(9):1059–1079.

35. Vinci P, Bastone A, Schiarea S, et al. Mesenchymal stromal cell-secreted chemerin is a novel immunomodulatory molecule driving the migration of ChemR23-expressing cells. *Cytotherapy*. 2017;19: 200-210.

36. Théry C, Amigorena S, Raposo G, Clayton A. Isolation and characterization of exosomes from cell culture supernatants and biological fluids. *Curr Protoc Cell Biol*. 2006;30:3.22.1-3.22.29.

37. Verderio C, Muzio L, Turola E, et al. Myeloid microvesicles are a marker and therapeutic target for neuroinflammation. *Ann Neurol*. 2012;72:610-624.

38. Li R, Shen Y. An old method facing a new challenge: re-visiting housekeeping proteins as internal reference control for neuroscience research. *Life Sci*. 2013;92:747-751.

39. Moritz CP. Tubulin or not tubulin: heading toward total protein staining as loading control in western blots. *Proteomics*. 2017;17: 1600189.

40. Das G, Reuhl K, Zhou R. The Golgi–Cox method. In: Zhou R, Mei L, eds. *Neural Development: Methods and Protocols*. Totowa, NJ: Humana Press; 2013:313-321.

41. Zaqout S, Kaindl AM. Golgi-Cox staining step by step. *Front Neuroanat*. 2016;10:38.

42. Gibb R, Kolb B. A method for vibratome sectioning of Golgi-Cox stained whole rat brain. *J Neurosci Methods*. 1998;79:1-4.

43. Pedrazzoli M, Losurdo M, Paolone G, et al. Glucocorticoid receptors modulate dendritic spine plasticity and microglia activity in an animal model of Alzheimer's disease. *Neurobiol Dis*. 2019;132:104568.

44. Dominici M, Le Blanc K, Mueller I, et al. Minimal criteria for defining multipotent mesenchymal stromal cells. The International Society for Cellular Therapy position statement. *Cytotherapy*. 2006;8: 315-317.

45. Tu Z, Li Q, Bu H, Lin F. Mesenchymal stem cells inhibit complement activation by secreting factor H. *Stem Cells Dev*. 2010;19:1803-1809.

46. François M, Romieu-Mourez R, Li M, Galipeau J. Human MSC suppression correlates with cytokine induction of indoleamine 2,3-dioxygenase and bystander M2 macrophage differentiation. *Mol Ther*. 2012;20:187-195.

47. Kota DJ, Prabhakara KS, Toledano-Furman N, et al. Prostaglandin E2 indicates therapeutic efficacy of mesenchymal stem cells in experimental traumatic brain injury. *Stem Cells*. 2017;35:1416-1430.

48. Imai Y, Ibata I, Ito D, Ohsawa K, Kohsaka S. A novel gene Iba1 in the major histocompatibility complex class III region encoding an EF hand protein expressed in a monocytic lineage. *Biochem Biophys Res Commun*. 1996;224:855-862.

49. Mastrangelo MA, Bowers WJ. Detailed immunohistochemical characterization of temporal and spatial progression of Alzheimer's disease-related pathologies in male triple-transgenic mice. *BMC Neurosci*. 2008;9:81.

50. Long Q, Upadhya D, Hattiangady B, et al. Intranasal MSC-derived A1-exosomes ease inflammation, and prevent abnormal neurogenesis and memory dysfunction after status epilepticus. *Proc Natl Acad Sci USA*. 2017;114:E3536-E3545.

51. Perry VH, Teeling J. Microglia and macrophages of the central nervous system: the contribution of microglia priming and systemic inflammation to chronic neurodegeneration. *Semin Immunopathol*. 2013;35:601-612.

52. Davis EJ, Foster TD, Thomas WE. Cellular forms and functions of brain microglia. *Brain Res Bull*. 1994;34:73-78.

53. Shi Q, Chowdhury S, Ma R, et al. Complement C3 deficiency protects against neurodegeneration in aged plaque-rich APP/PS1 mice. *Sci Transl Med*. 2017;9:eaaf6295.

54. Rajendran L, Paolicelli RC. Microglia-mediated synapse loss in Alzheimer's disease. *J Neurosci*. 2018;38:2911-2919.

55. Koniusz S, Andrzejewska A, Muraca M, et al. Extracellular vesicles in physiology, pathology, and therapy of the immune and central nervous system, with focus on extracellular vesicles derived from mesenchymal stem cells as therapeutic tools. *Front Cell Neurosci*. 2016;10:109.

56. Maggini J, Mirkin G, Bognanni I, et al. Mouse bone marrow-derived mesenchymal stromal cells turn activated macrophages into a regulatory-like profile. *PLoS One*. 2010;5:e9252.

57. Griffin WS, Stanley LC, Ling C, et al. Brain interleukin 1 and S-100 immunoreactivity are elevated in Down syndrome and Alzheimer disease. *Proc Natl Acad Sci USA*. 1989;86:7611-7615.

58. Licastro F, Pedrini S, Caputo L, et al. Increased plasma levels of interleukin-1, interleukin-6 and α-1-antichymotrypsin in patients with Alzheimer's disease: peripheral inflammation or signals from the brain? *J Neuroimmunol*. 2000;103:97-102.

59. Lim S-H, Park E, You B, et al. Neuronal synapse formation induced by microglia and interleukin 10. *PLoS One*. 2013;8:e81218.

60. Jaimes Y, Naaldijk Y, Wenk K, et al. Mesenchymal stem cell-derived microvesicles modulate lipopolysaccharides-induced inflammatory responses to microglia cells. *Stem Cells*. 2016;35: 812-823.

61. Harting MT, Srivastava AK, Zhaorigetu S, et al. Inflammation-stimulated mesenchymal stromal cell-derived extracellular vesicles attenuate inflammation. *Stem Cells*. 2018;36:79-90.

62. Sasaki Y, Ohsawa K, Kanazawa H, Kohsaka S, Imai Y. Iba1 is an actin-cross-linking protein in macrophages/microglia. *Biochem Biophys Res Commun*. 2001;286:292-297.

63. Marzolo MP, von Bernhardi R, Inestrosa NC. Mannose receptor is present in a functional state in rat microglial cells. *J Neurosci Res*. 1999;58:387-395.

64. Durafourt BA, Moore CS, Zammit DA, et al. Comparison of polarization properties of human adult microglia and blood-derived macrophages. *Glia*. 2012;60:717-727.

65. Chhor V, Le Charpentier T, Lebon S, et al. Characterization of phenotype markers and neuronotoxic potential of polarised primary microglia in vitro. *Brain Behav Immun*. 2013;32:70-85.

66. Hammond TR, Dufort C, Dissing-Olesen L, et al. Single-cell RNA sequencing of microglia throughout the mouse lifespan and in the injured brain reveals complex cell-state changes. *Immunity*. 2019;50: 253-271.

67. Matcovitch-Natan O, Winter DR, Giladi A, et al. Microglia development follows a stepwise program to regulate brain homeostasis. *Science*. 2016;353(6301):aad8670-1–aad8670-12.

68. Prockop DJ. Concise review: two negative feedback loops place mesenchymal stem/stromal cells at the center of early regulators of inflammation. *Sᴛᴇᴍ Cᴇʟʟꜱ*. 2013;31:2042-2046.

69. Kushima Y, Hama T, Hatanaka H. Interleukin-6 as a neurotrophic factor for promoting the survival of cultured catecholaminergic neurons in a chemically defined medium from fetal and postnatal rat midbrains. *Neurosci Res*. 1992;13:267-280.

70. Oh J, McCloskey MA, Blong CC, Bendickson L, Nilsen-Hamilton M, Sakaguchi DS. Astrocyte-derived interleukin-6 promotes specific neuronal differentiation of neural progenitor cells from adult hippocampus. *J Neurosci Res*. 2010;88:2798-2809.

71. Sato A, Ohtaki H, Tsumuraya T, et al. Interleukin-1 participates in the classical and alternative activation of microglia/macrophages after spinal cord injury. *J Neuroinflammation*. 2012;9:1-17.

72. Kowsar R, Keshtegar B, Miyamoto A. Understanding the hidden relations between pro- and anti-inflammatory cytokine genes in bovine oviduct epithelium using a multilayer response surface method. *Sci Rep*. 2019;9:1-17.

73. Fitzgerald W, Freeman ML, Lederman MM, et al. A system of cytokines encapsulated in extracellular vesicles. *Sci Rep*. 2018;8: 1-11.

74. Zilka N, Zilkova M, Kazmerova Z, Sarissky M, Cigankova V, Novak M. Mesenchymal stem cells rescue the Alzheimer's disease cell model from cell death induced by misfolded truncated tau. *Neuroscience*. 2011;193:330-337.

75. Lee HJ, Lee JK, Lee H, et al. Human umbilical cord blood-derived mesenchymal stem cells improve neuropathology and cognitive impairment in an Alzheimer's disease mouse model through modulation of neuroinflammation. *Neurobiol Aging*. 2012;33:588-602.

76. Yun H-M, Kim HS, Park K-R, et al. Placenta-derived mesenchymal stem cells improve memory dysfunction in an Aβ(1–42)-infused mouse model of Alzheimer's disease. *Cell Death Dis*. 2013;4:e958.

77. Yang H, Xie Z, Wei L, et al. Human umbilical cord mesenchymal stem cell-derived neuron-like cells rescue memory deficits and reduce amyloid-beta deposition in an AβPP/PS1 transgenic mouse model. *Stem Cell Res Ther*. 2013;4:76.

78. Zhao Y, Chen X, Wu Y, Wang Y, Li Y, Xiang C. Transplantation of human menstrual blood-derived mesenchymal stem cells alleviates Alzheimer's disease-like pathology in APP/PS1 transgenic mice. *Front Mol Neurosci*. 2018;11:140.

79. Oh SH, Kim HN, Park H-J, Shin JY, Lee PH. Mesenchymal stem cells increase hippocampal neurogenesis and neuronal differentiation by enhancing the Wnt signaling pathway in an Alzheimer's disease model. *Cell Transplant*. 2015;24:1097-1109.

80. Naaldijk Y, Jäger C, Fabian C, et al. Effect of systemic transplantation of bone marrow-derived mesenchymal stem cells on neuropathology markers in APP/PS1 Alzheimer mice. *Neuropathol Appl Neurobiol*. 2016;43:299-314.

81. Lener T, Gimona M, Aigner L, et al. Applying extracellular vesicles based therapeutics in clinical trials – an ISEV position paper. *J Extracell Vesicles*. 2015;4:30087–30107. https://doi.org/10.3402/jev.v4.30087

82. Narbute K, Piļipenko V, Pupure J, et al. Intranasal administration of extracellular vesicles derived from human teeth stem cells improves motor symptoms and normalizes tyrosine hydroxylase expression in the substantia nigra and striatum of the 6-hydroxydopamine-treated rats. *Sᴛᴇᴍ Cᴇʟʟꜱ ᴛʀᴀɴꜱʟᴀᴛɪᴏɴᴀʟ Mᴇᴅɪᴄɪɴᴇ*. 2019;8:490-499.

83. Kodali M, Castro WO, Kim D-K, et al. Intranasally administered human MSC-derived extracellular vesicles pervasively incorporate into neurons and microglia in both intact and status epilepticus injured forebrain. *Int J Mol Sci*. 2020;21:181–195.

84. Zhuang X, Xiang X, Grizzle W, et al. Treatment of brain inflammatory diseases by delivering exosome encapsulated anti-inflammatory drugs from the nasal region to the brain. *Mol Ther*. 2011;19:1769-1779.

85. Perets N, Hertz S, London M, Offen D. Intranasal administration of exosomes derived from mesenchymal stem cells ameliorates autistic-like behaviors of BTBR mice. *Mol Autism*. 2018;9:57.

86. Reza-Zaldivar EE, Hernández-Sapiéns MA, Gutiérrez-Mercado YK, et al. Mesenchymal stem cell-derived exosomes promote neurogenesis and cognitive function recovery in a mouse model of Alzheimer's disease. *Neural Regen Res*. 2019;14: 1626-1634.

87. Oddo S, Caccamo A, Shepherd JD, et al. Triple-transgenic model of Alzheimer's disease with plaques and tangles: intracellular Aβ and synaptic dysfunction. *Neuron*. 2003;39:409-421.

88. Janelsins MC, Mastrangelo MA, Oddo S, LaFerla FM, Federoff HJ, Bowers WJ. Early correlation of microglial activation with enhanced tumor necrosis factor-alpha and monocyte chemoattractant protein-1 expression specifically within the entorhinal cortex of triple transgenic Alzheimer's disease mice. *J Neuroinflammation*. 2005; 2:23.

89. Rodríguez JJ, Witton J, Olabarria M, Noristani HN, Verkhratsky A. Increase in the density of resting microglia precedes neuritic plaque formation and microglial activation in a transgenic model of Alzheimer's disease. *Cell Death Dis*. 2010;1:e1.

90. McGeer PL, Itagaki S, Tago H, et al. Reactive microglia in patients with senile dementia of the Alzheimer type are positive for the histocompatibility glycoprotein HLA-DR. *Neurosci Lett*. 1987;79: 195-200.

91. Jimenez S, Baglietto-Vargas D, Caballero C, et al. Inflammatory response in the hippocampus of PS1M146L/APP751SL mouse model of Alzheimer's disease: age-dependent switch in the microglial phenotype from alternative to classic. *J Neurosci*. 2008;28:11650-11661.

92. Fyfe I. Blocking microglial proliferation halts Alzheimer disease in mice. *Nat Rev Neurol*. 2016;12:64.

93. Olmos-Alonso A, Schetters STT, Sri S, et al. Pharmacological targeting of CSF1R inhibits microglial proliferation and prevents the progression of Alzheimer's-like pathology. *Brain*. 2016;139: 891-907.

94. Gate D, Rezai-Zadeh K, Jodry D, Rentsendorj A, Town T. Macrophages in Alzheimer's disease: the blood-borne identity. *J Neural Transm*. 2010;117:961-970.

95. Thériault P, Elali A, Rivest S. The dynamics of monocytes and microglia in Alzheimer's disease. *Alzheimers Res Ther*. 2015;7: 1-10.

96. Henao Agudelo JS, Braga TT, Amano MT, et al. Mesenchymal stromal cell-derived microvesicles regulate an internal pro-inflammatory program in activated macrophages. *Front Immunol*. 2017;8:881.

97. Unger MS, Schernthaner P, Marschallinger J, et al. Microglia prevent peripheral immune cell invasion and promote an anti-inflammatory environment in the brain of APP-PS1 transgenic mice. *J Neuroinflammation*. 2018;15:1-23.

98. Pellicanò M, Larbi A, Goldeck D, et al. Immune profiling of Alzheimer patients. *J Neuroimmunol*. 2012;242:52-59.

99. Baruch K, Rosenzweig N, Kertser A, et al. Breaking immune tolerance by targeting Foxp3+ regulatory T cells mitigates Alzheimer's disease pathology. *Nat Commun*. 2015;6:7967.

100. Marsh SE, Abud EM, Lakatos A, et al. The adaptive immune system restrains Alzheimer's disease pathogenesis by modulating microglial function. *Proc Natl Acad Sci USA*. 2016;113(9):E1316-E1325.

101. Zanier ER, Pischiutta F, Riganti L, et al. Bone marrow mesenchymal stromal cells drive protective M2 microglia polarization after brain trauma. *Neurotherapeutics*. 2014;11:679-695.

102. Bodart-Santos V, De Carvalho LRP, De Godoy MA, et al. Extracellular vesicles derived from human Wharton's jelly mesenchymal stem cells protect hippocampal neurons from oxidative stress and synapse damage induced by amyloid-β oligomers. *Stem Cell Res Ther*. 2019;10:1-13.

103. de Godoy MA, Saraiva LM, de Carvalho LRP, et al. Mesenchymal stem cells and cell-derived extracellular vesicles protect hippocampal neurons from oxidative stress and synapse damage induced by amyloid-β oligomers. *J Biol Chem*. 2018;293:1957-1975.

104. Ransohoff RM, Cardona AE. The myeloid cells of the central nervous system parenchyma. *Nature*. 2010;468:253-262.

105. Tong L, Prieto GA, Kramár EA, et al. Brain-derived neurotrophic factor-dependent synaptic plasticity is suppressed by interleukin-1β via p38 mitogen-activated protein kinase. *J Neurosci*. 2012;32:17714-17724.

106. Hong S, Beja-Glasser VF, Nfonoyim BM, et al. Complement and microglia mediate early synapse loss in Alzheimer mouse models. *Science*. 2016;352:712-716.

107. Haney MJ, Klyachko NL, Zhao Y, et al. Exosomes as drug delivery vehicles for Parkinson's disease therapy. *J Control Release*. 2015;207:18-30.

SUPPORTING INFORMATION

Additional supporting information may be found online in the Supporting Information section at the end of this article.